Optic Radiations Microstructural Changes in Glaucoma and Association With Severity: A Study Using 3Tesla-Magnetic Resonance Diffusion Tensor Imaging

Laury Tellouck, Muriel Durieux, Pierrick Coupé, Audrey Cougnard-Grégoire, Joy Tellouck, Thomas Tourdias, Fanny Munsch, Arnaud Garrigues, Catherine Helmer, Florence Malet, et al.

OPTIC RADIATIONS MICROSTRUCTURAL CHANGES IN GLAUCOMA AND ASSOCIATION WITH SEVERITY: A STUDY USING 3TESLA-MAGNETIC RESONANCE DIFFUSION TENSOR IMAGING

Laury Tellouck[1,2,3], Muriel Durieux [4], Pierrick Coupé [5,6], Audrey Cougnard-Grégoire[2,3], Joy Tellouck[1], Thomas Tourdias [2,4,7], Fanny Munsch [4]; Arnaud Garrigues [1], Catherine Helmer [2,3], Florence Malet[8], Jean-François Dartigues [2,3], Vincent Dousset [2,4,7], Cécile Delcourt[2,3], Cédric Schweitzer[1,2,3]

1: CHU de Bordeaux, Service d'Ophtalmologie, F-33000 Bordeaux, France.

2: Univ. Bordeaux, F-33000 Bordeaux, France.

3: INSERM, U1219 - Bordeaux Population Health Research Center, F-33000 Bordeaux, France.

4: CHU de Bordeaux, Service de Neuro-Imagerie, F-33000 Bordeaux, France.

5: Université de Bordeaux, LaBRI, UMR 5800, PICTURA, F-33400 Talence, France.

6: CNRS, LaBRI, UMR 5800, PICTURA, F-33400 Talence, France.

7 : INSERM U1215, Neurocentre Magendie, F-33000 Bordeaux, France.

8: Centre d'Ophtalmologie Point Vision, F-33000 Bordeaux, France.

Corresponding author/reprint request: Cécile Delcourt, Inserm U1219, ISPED, 146 rue Léo Saignat, 33076 Bordeaux Cedex. Tel: + 33 557 57 11 91. Email: cecile.delcourt@isped.fr

Word count: 4089

Financial support: This study received financial support from UNADEV (Bordeaux, France). UNADEV did not participate in the design of the study, the collection, management, statistical analysis and interpretation of the data, nor in the preparation, review or approval of the present manuscript.

ABSTRACT

Purpose:

To compare microstructural changes along the optical radiations and brain structure volumes between glaucoma and control subjects using in vivo magnetic resonance imaging and to analyze their association with severity of the disease.

Methods: 50 open-angle glaucoma subjects and 50 healthy age- and sex-matched controls underwent detailed ophthalmological examinations (including visual field testing (VF), funduscopy and Spectral-Domain Optical Coherence Tomography) as well as Diffusion tensor imaging (DTI) using a 3.0-Tesla MRI. Fractional anisotropy (FA), Mean Diffusivity, Radial Diffusivity (RD) and Axial Diffusivity (AD) were quantified semi-automatically along the optical radiations. DTI parameters and volumes of specific brain structures were compared between cases and controls using conditional logistic regression. Association between DTI metrics and the severity of the disease was studied using linear mixed regression analyses.

Results: In glaucoma subjects, optic radiations FA was significantly lower (0.57 vs 0.59; p= 0.02) and RD was significantly higher (52.78 10^{-5} mm^2/s vs 49.74 10^{-5} mm^2/s; p= 0.03) than in controls. Optic radiations FA was significantly correlated with homolateral functional and structural damage of glaucoma (mean deviation of VF (p=0.03), retinal nerve fiber layer thickness (p=0.03), vertical cup/disc ratio (p=0.0007)). Volume and DTI parameters of other brain structures (including hippocampus) were not significantly different between glaucoma and controls.

Conclusion: We evidenced microstructural modifications along visual pathways of glaucoma patients and these alterations were correlated with disease severity. The association of glaucoma with other neurodegenerative alterations would need further exploration and a prospective follow-up of our cohort of subjects.

Keywords: glaucoma, fractional anisotropy, 3T MRI, optic radiations, DTI

INTRODUCTION

Glaucoma affects 64 million people and is the first cause of irreversible blindness, worldwide[1,2]. It encompasses a group of disorders characterized by progressive degeneration of the optic nerve head, loss of retinal ganglion cells and a corresponding pattern of visual field loss[3]. Primary open-angle glaucoma (POAG) is the predominant form of glaucoma in Western countries. Although some risk factors for POAG have been identified (high intraocular pressure, age, high myopia, ethnicity and heredity), several aspects of its pathophysiology remain unclear. As the disease could also affect intra-cerebral visual pathways in addition to optic nerve head degeneration, a neurodegenerative hypothesis raises concerns[4,5]

Central visual pathway degeneration in glaucoma was first suggested in experimental and histological studies, which have evidenced that glaucoma is not strictly limited to the optic nerve[6,7]. In an animal model of ocular hypertension, brain changes were observed in the lateral geniculate nucleus and superior colliculus, in parallel with retinal ganglion cells loss[8]. In another study, grey matter of glaucoma patients was reduced compared to healthy subjects, in the approximate retinal lesion projection zones in the visual cortex[9]. Moreover, a clinicopathological case in humans highlighted a neural degeneration in intracranial optic nerve, lateral geniculate nucleus and visual cortex[10]. This paradigmatic shift is further supported by several other small-sized clinical studies using brain magnetic resonance imaging, showing reduced volume of all the visual pathways (optic tracts, optic chiasm, lateral geniculate nucleus, optic radiations) measured at 1.5T[11–13] or 3T field strength[14,15].

Some other experimental studies may help understand the pathogenesis of the disease. Using in vivo MRI studies is a way to study metabolic and spatiotemporal changes in glaucoma[16–18].

In addition, epidemiological studies have also suggested that glaucoma might be associated with other neurodegenerative disorders, in particular Alzheimer's disease[19,20], and a few studies have found a reduced volume of brain structures, beyond the visual pathways – particularly in the hippocampus – which is well known to be affected in Alzheimer's disease[14,21,22]. These data have nevertheless been collected in patients with long standing disease. Whether subtle alterations suggestive of associated neurodegenerative disease can be captured from the early stage of glaucoma, prior to atrophy, is unknown.

Recent improvements in neuroimaging techniques allow more accurate evaluation of brain structure volumes and intra-cerebral microstructural damage. By quantifying microscopic movements of water molecules, Diffusion Tensor Imaging (DTI) – a functional MRI technique – provides a sensitive evaluation of underlying brain microstructural changes even prior to atrophy[23]. Therefore, this technique appears particularly promising in the documentation of intra-cerebral damage in glaucoma. The most commonly assessed DTI parameters include fractional anisotropy (FA, which reflects the degree of cellular structural alignment within fiber tracts and the structural integrity of the fiber tracts) and mean diffusivity (MD, which measures the average motion of water molecules independently of fiber directionality).

Several case-control studies have already shown that FA of the optic radiations is decreased and MD increased in glaucoma patients[24,25], and some others have suggested that these changes may be progressive with increasing axon loss of the

optic nerve[26]. Whereas these studies provide new insights in the understanding of glaucoma disease, they were limited in sample size and mainly included advanced glaucoma patients.

Therefore, our study aimed at exploring the potential neurodegenerative hypothesis associated with glaucoma and whether subtle changes could be measurable at the early stage of the disease. Thus we analyzed both the microstructural changes of the visual pathway, in relation with glaucoma severity, as well as changes beyond the visual pathway, in particular in regions affected in neurodegenerative pathologies.

METHODS

Patient Population

This study is an observational case-control study performed at the University Hospital of Bordeaux. Fifty patients with POAG (20 men, 30 women, mean age 61.9 +/- 6.9 years) and 50 age- and sex-matched controls (20 men, 30 women, mean age 61.9 +/- 7.0 years) were prospectively included.

This research followed the tenets of the Declaration of Helsinki. Participants gave written consent for the participation in the study. The design of this study was approved by the Ethical Committee of Bordeaux (Comité de Protection des Personnes Sud-Ouest et Outre-Mer III) in March 2012. This study was registered on the website http://clinicaltrials.gov/ (identifier NCT01621841).

Ophthalmological Examination

All participants underwent a complete ophthalmic examination including measurement of best-corrected visual acuity, intraocular pressure (IOP) using Goldmann aplanation

tonometry, gonioscopy, slit-lamp biomicroscopy and optic disc examination by funduscopy. Central corneal thickness and anterior chamber depth were assessed using interferometry (OCT Visante, Carl Zeiss Meditec, Inc., Dublin, CA, USA), and axial length measurement using IOL Master (Carl Zeiss Meditec, Inc., Dublin, CA, USA). All participants underwent a visual field testing (Octopus 101, Haag-Streit, Inc., Bern, Switzerland) and only reliable tests (false-positive errors <15%, false negative-errors <15%, loss fixations <20%) were included. In addition, visual fields (VF) were reviewed and excluded in the presence of artefacts, such as eyelid or rim artifacts, fatigue effects, inattention, or inappropriate fixation.

A measurement of peripapillary Retinal Nerve Fiber Layer (RNFL) thickness was performed using Spectral-Domain optical coherence tomography (SD-OCT) (Cirrus, Carl Zeiss Meditec, Inc., Dublin, CA, USA). All images were acquired and reviewed by specially trained technicians of the study to control the quality of signal strength and accurate centration and segmentation of the RNFL circle scan acquisition. Signal strength lower than 6 or acquisitions with artifacts were excluded from the analysis.

Glaucoma subjects and controls received a questionnaire requesting for cardiovascular risk factors, familial history of glaucoma, ophthalmological diseases and current medications. Each participant underwent Mini Mental State Examination (MMSE)[27].

Primary open-angle glaucoma was defined by the following criteria: the presence of glaucomatous optic neuropathy (defined as a loss of neuroretinal rim with a vertical cup-to-disc ratio [VCDR] of >0.7 or an intereye asymmetry of >0.2, with or without notching attributable to glaucoma) associated to compatible VF loss. This VF loss was defined as the presence of at least 3 contiguous non edge test points within the same

hemifield on the pattern deviation probability plot at $P < 0.05$, with at least 1 point $P < 0.01$, excluding points directly above and below the blind spot, and the presence of glaucomatous hemifield test results outside normal limits. Iridocorneal angle opening was graded 3 or 4 on gonioscopy using Schaeffer classification.

Controls were defined as normal optic disc without notching or abnormal thinning of the neuroretinal rim, no visual field defects, IOP measurement < 21 mmHg and no family history of glaucoma.

Exclusion criteria included any diseases that could affect the visual field, secondary glaucoma including exfoliative and pigmentary glaucoma, diabetes mellitus, any neurological or psychiatric disorders, and a score <26 on the MMSE for global cognition. We also excluded participants according to standard MRI exclusion criteria such as claustrophobia, ferromagnetic implants or pacemakers, and inability to lie still for the MRI acquisition time.

Stage of severity of glaucoma was classified according to the Hodapp-Parrish-Anderson classification[28]. The different stages are:

- Stage 0: no or minimal defect
- Stage 1: MD ≥ -6.0 dB (early defect)
- Stage 2: -12.0 ≥ MD ≥ -6.0 dB (moderate defect)
- Stage 3: -20 ≥ MD ≥ -12.0 dB (advanced defect)
- Stage 4: MD ≥ - 20.0 dB (severe defect)
- Stage 5: End-stage disease

MRI Data Acquisition

MRI examinations were performed on a 3-T Discovery MR750w scanner (GE Medical Systems, Milwaukee, WI, USA) using a 32-channel phased array head coil within 30 days following the ophthalmologic examinations. The protocol included a DTI sequence to look for microstructural alterations along and beyond the optic radiations, a 3D-T1-wi sequence to look for global or focal atrophy. The parameters of acquisitions were as follows. The DTI sequence consisted in dual echo-planar imaging: 40 axial slices; repetition time, 12000 ms; echo time, 100.9 ms; slice thickness, 3.5 mm; matrix, 160x160; field of view, 24 cmx24 cm; b values, 0 and 1000 s/mm² applied in 32 non-collinear directions. The 3D-T1 was an inversion recovery gradient echo sequence: 288 slices; repetition time, 11.4 ms; echo time, 4.3 ms; inversion time, 400 ms; flip angle, 15°; slice thickness, 0.8 mm; matrix, 384x384; field of view, 25 cmx25 cm.

Image Processing

Measurement of DTI metrics along the optic radiations

From the DTI data, the distortions induced by eddy currents were first corrected, then a diffusion tensor model was fitted at each voxel using Olea Medical® software to generate fractional anisotropy (FA) maps and to investigate the microstructural integrity of the optic radiations. The optic radiations were identified using deterministic tractography between two seed-regions of interest (ROIs) over the proximal and distal optic radiations according to previously published method and landmarks[29]. The proximal ROI was placed near the lateral geniculate nuclei, while the distal ROI was placed just anterior to its termination in the visual cortex. Fiber tract propagation was terminated for FA<0.2 and angle<35° based on agreed-upon thresholds. ROIs were placed by a specialized neuroradiologist symetrically, based on color-coded FA maps

and trace DTI images on the anterior and posterior part of the expected pathway of the optic radiations (green boxes on Figure 1). Fibers whose directions did not correspond to the optic radiations based on anatomic knowledge and DTI-derived atlas were excluded by adding additional ROIs and a logical "not" function[30] (red boxes on Figure 1). Only fibers that connected the anterior and posterior regions of interest were selected for further analysis. The analysis was independently repeated for a subset of cases (n=25 out of the 100 cases) by a specialized ophthalmologist with an inter-reader agreement of 0.88.

The median FA and its sub-component (axial and radial diffusivity, AD and RD respectively) as well as the mean diffusivity were measured along the reconstructed optic radiations (green streamlines on Figure 1). Decreased FA and increased MD values is usually considered as a proxy of axonal disruption[31].

None of the people participating in FA measurements had any access to the case/control status of the participants, nor to any other clinical data.

MRI volumetric measurements

For volumetric analyses, T1-weighted images were processed using the volBrain system (http://volbrain.upv.es). After denoising[32], images were affine-registered[33] into the Montreal Neurological Institute space and the total brain volume was estimated using the Nonlocal Intracranial Cavity Extraction method[34]. Hippocampus was segmented using patch-based multi-template approach[35] following the international consortium from the EADC-ADNI Harmonized Protocol for anatomical definitions of the hippocampus[36]. To control variations in head size between subjects, total brain volumes and hippocampal volumes were scaled using the volumetric scaling factor determined through the affine registration to the MNI brain template.

For DTI analysis within the hippocampus masks, an in-house pipeline (dtiBrain) was used to process diffusion-weighted images. First, diffusion-weighted images were affine-registered to the T1w MRI in the MNI space[32]. Then, to compensate for EPI distortion, a non-rigid registration was performed. Finally, a diffusion tensor model was fitted at each voxel using FSL 5.031 (fmrib.ox.ac.uk/fsl), generating FA and MD maps. Mean FA and MD were measured within the hippocampal masks previously generated on anatomical T1-weighted MRI.

Statistical analysis

Statistical analysis was performed using SAS 9.3 (SAS Institute Inc, Cary, NC). Differences of MRI characteristics between glaucoma subjects and healthy controls were tested using logistic conditional analyses, for parameters both along optic radiations and outside the visual pathway (globally for white and grey matter and in hippocampal and amygdala structures). Additionally, within the group of patients with glaucoma, we used mixed linear regression analyses, adjusted for sex and age (as a continuous variable expressed in years), to test the associations between optic radiation DTI parameters (FA, MD, AD, RD) and the parameters of severity of the disease (VCDR, mean deviation of VF and RNFL). This type of analysis allows taking into account both right and left sides of each patient, while taking into account the intra-individual correlation between sides. In particular, this allowed studying the associations of ocular parameters with homolateral (right optic radiation with right eye and left with left eye) and contralateral (right optic radiation with left eye and vice versa) optic radiations MRI parameters. In these regression analyses, both ocular and

brain parameters were entered as z-scores. In addition, for RNFL, we also adjusted for axial length, which is strongly associated with RNFL[37].

RESULTS

Demographic and ophthalmological characteristics

As shown in Table 1, cases and controls were similar for age, gender, history of cardiovascular diseases or risk factors and MMSE. Family history of glaucoma was reported by 58 % of glaucoma patients, and 0 % of controls (since this was an exclusion criterion for controls).

As shown in Table 2, cases and controls did not significantly differ for visual acuity (distance and near), intraocular pressure and axial length. As expected, they were significantly different for central corneal thickness, VCDR, RNFL thickness and visual field parameters. Similar results were observed for the left eye (Table 3).

In our study, 70% of glaucoma patients had an early stage of the disease, 20% a moderate stage and 10% an advanced or severe stage, according to the Hodapp-Parrish-Anderson classification.

Comparison of MRI parameters along optic radiations between glaucoma and control subjects

One patient refused to do MRI examination and 3 MRI examinations were insufficient quality for analysis, leaving 49 glaucoma patients and 47 controls for the comparison of MRI parameters (Table 4). The optic radiations were similarly reconstructed for glaucoma and control subjects (similar length and volume and reconstructed streamlines). Glaucoma patients showed significantly lower FA along the optic radiations than controls (0.57 vs 0.59, p=0.02), which was driven by significant

increase in radial diffusivity (52.8 10^{-5} mm^2/s vs 49.7 10^{-5} mm^2/s, p=0.03) while axial diffusivity was unchanged. Mean diffusivity tended to be slightly higher in glaucoma patients, but this did not reach statistical significance (82.4 10^{-5} mm^2/s vs 80.6 10^{-5} mm^2/s p=0.10).

Associations of homo- and contralateral optic radiation parameters with the severity of the disease in glaucoma patients

Table 5 shows the associations of optic radiation parameters (FA, MD, RD and AD) with the ophthalmological parameters of glaucoma severity evaluated by visual field, optic disc cupping and RNFL thickness, only among patients with glaucoma (n=50). We tested associations of ophthalmological parameters with MRI parameters on the homolateral (right eye – right optic radiation and left eye – left optic radiation) and contralateral (right-left and left-right) sides. For the homolateral side, significant associations were found between optic radiations FA and mean deviation of the visual field (β= -0.22; p= 0.03), VCDR (β= -0.42; p= 0.0003) and RNFL (β= 0.22; p= 0.03). The direction of the association is opposite for RNFL, since RNFL decreases with higher severity of glaucoma, while other parameters increase with severity. Mean and radial diffusivities increased with the severity of the disease measured by VCDR, ($p<0.006$ and $p<0.0008$, respectively), but were not significantly associated with mean deviation of VF or RNFL thickness. By contrast, axial diffusivity, as well as length and volume of optic radiations were not significantly associated with any of the severity parameters.

With regard to the contralateral side, associations of MRI parameters with glaucoma severity parameters were much weaker, and reached statistical significance only for the association of FA and RD with VCDR (p=0.01 and p=0.02, respectively).

Brain volumes analyses between cases and controls

Finally, we did not evidence any statistically significant difference between glaucoma subjects and controls for volumes and DTI parameters of cerebrum white and grey matters, hippocampus and amygdala (Table 6).

DISCUSSION

Our study demonstrates microstructural changes of the optic radiations in glaucoma, as evaluated by lower FA driven by higher RD, and a correlation between the level of structural modifications and disease severity.

Using MRI at 1.5T[38] or 3T[25,26,39] a few case-control studies have also reported such modifications of diffusion parameters in optic radiations of glaucoma patients. All these studies found significantly lower FA in glaucoma patients compared with control patients. In the present study, which included 70 % of early stages of glaucoma, FA differences between cases and controls are numerically small (about 0.02 for a mean of about 0.60, i.e about 3.3 %). However, the standard deviation is also small (about 0.04), showing low inter-individual variability in this parameter, and the difference is substantial when related to the standard deviation (about 0.5 SD), suggesting a major effect of glaucoma on this highly conserved parameter. In other studies, the differences in FA of optic radiations observed between glaucoma patients and controls were larger, but these studies generally included more severe cases. The study by Engelhorn et al included 22 severe glaucoma cases, and observed a difference in FA of optic radiations ranging from 17 % to 30 % according to the localization (anterior, central, posterior)[39]. The study by Murai et al included 18 severe glaucoma cases, 9 moderate and only 2 mild, and observed a 14 % difference in FA of the optic

radiations[38]. The study by Garaci et al included 4 pre-perimetric glaucoma cases, 4 early, 4 moderate and 4 severe cases and observed a 36 % differences in FA of the optic radiations[25]. Finally, the study by Chen et al included a majority of severe cases (36 eyes with MD>9.5 dB out of 50) but did not report numerically the averages of optic radiations FA[26].

Furthermore, we observed higher RD value in glaucoma patients and its correlation with disease severity whereas AD was not significantly different between glaucoma and control patients. Although, AD and RD are the two components of FA, these parameters have been scarcely analyzed in the literature and some studies have already reported increasing RD in glaucoma subjects compared to controls[24].

Even though the underlying pathological alterations are not specifically known, animal studies have suggested that higher RD could mainly represent myelin loss while lower AD could be a more specific marker of neuronal loss. However these considerations were based on simplistic models and whether alterations of optic radiations truly predominate on myelin or axon component cannot be formally ascertained for glaucoma patients, for whom other modifications such as microglia activation may confound the data.

Additionally, we observed a trend towards higher mean diffusivity value in the glaucoma group without reaching statistical significance. However, we observed a significant positive correlation between mean diffusivity and disease severity measured with VCDR. Two studies also showed higher mean diffusivity in glaucoma patients[25,26]. While FA measures the degree of cellular structural alignment within fiber tracts and their structural integrity, mean diffusivity measures the average motion of water molecules independently of fiber directionality and is considered as an additional marker of axonal disruption. As these studies included patients with advanced

370 glaucoma, our findings might be explained by a lack of statistical power and a lower
371 grade of disease severity in our glaucoma group. Such converging evidence of loss of
372 fiber integrity in optic radiations in glaucoma cannot be measured in terms of length
373 and volume of the optic radiations, which were similar in both groups probably
374 because our measurements were made prior to fiber loss or major disorganization.
375
376 We also observed an association of diffusivity parameters (mainly FA and RD), with
377 the severity of glaucoma (assessed by mean deviation of the visual field, VCDR and
378 RNFL measured with SD-OCT), suggesting that microstructural changes to the optic
379 radiations is one of the components of the severity that could participate in the
380 clinical status of the patients and the alteration of the visual field. Although we mainly
381 included early and moderate glaucoma as defined by the Hodapp-Parrish-Anderson
382 classification, our findings are consistent with some previous studies, which included
383 more advanced cases[26,38–40]. All these studies also evidenced significant
384 associations of optic radiations FA with structural parameters of optic nerve head
385 degeneration evaluated with VCDR or time-domain RNFL thickness, as well as
386 functional visual field alterations. For example, Michelson *et al.* found a correlation
387 between FA and visual field[40]. Thus, all these results illustrate the fact that FA could
388 be a strong biomarker of glaucoma severity.
389 Our study also assessed the associations of glaucoma severity according to FA of
390 homolateral and contralateral optic radiations. Interestingly, glaucoma severity
391 parameters – in particular VCDR – were more strongly associated with homolateral
392 optic radiations diffusion parameters than with contralateral parameters. As chiasmatic
393 decussation of optic pathways results in approximately 50% crossing of axons on the
394 contralateral side[41], we would expect similar associations of glaucoma severity

parameters with homolateral and contralateral diffusion parameters. However, our findings might also be related to an increased vulnerability of some specific retinal nerve fiber bundles of the optic nerve head resulting in an atrophy of optic radiations more predominant on the homolateral side of the decussation than on the controlateral. Indeed, several studies have demonstrated a specific vulnerability of the temporal and temporal-inferior sides of the optic nerve head to glaucoma damage[42–44]. Thus, we could expect an increased atrophy of the corresponding optic radiation predominant on the homolateral side that could explain our findings. However, even if temporal and temporal-inferior nerve fiber layers are more vulnerable to glaucomatous damage, the meaning of our findings should be interpreted with caution and would need further exploration to be confirmed and to identify the exact underlying mechanism. Indeed, distribution of RNFL is not homogeneous around the optic nerve head with superior and inferior sectorial RNFL thicker than nasal or temporal RNFL sectors. Furthermore the mean optic disc-fovea angle deliminating superior and inferior nerve fiber layers, is around 8°[45]. Thus the exact distribution of nerve fiber layers of the retina that decussates to the contralateral optic tract or remains on the ipsilateral optic tract and finally leads to a vertical delimitation through the fovea on the hemivisual field test remains unclear. Hence, in our study, the corresponding optic radiations in the homo or contralateral side could not be accurately matched to specific sectors of the retina or the optic nerve head.

Although high intraocular pressure is the main risk factor of glaucoma, this disease is increasingly considered as a neuro-ophthalmological and neurodegenerative disease[46]. Furthermore, there are still controversies on the association between glaucoma and some other neurodegenerative diseases as Alzheimer's disease. In particular, in a cohort of elderly subjects followed every 2 years, we observed an

association of POAG with incident dementia[19]. Volume changes beyond the visual system in glaucoma patients have also been reported in several studies but with inconsistent results. For instance, Frezzotti *et al.* reported that POAG patients had brain atrophy in some grey matter regions and the visual cortex[21]. By contrast, Williams *et al.* found five cerebral structures larger in the glaucoma group than in the control group[22]. Chen *et al.* revealed both a decreasing grey matter volume in some regions and an increasing grey matter volume in some others[14]. In the present study, we analyzed brain globally and focused on brain regions that are well known to be affected in the course of Alzheimer's disease – particularly hippocampus – and did not evidence any significant difference for any of the studied regions of interest, neither in volume nor in parameters of diffusivity. However, as we included subjects with MMSE ≥26 at baseline, the risk of brain structures atrophy was probably limited. Regarding the hippocampus, results have been particularly inconsistent, since Frezzotti *et al.* reported decreased hippocampus volume in glaucoma patients[21], while Williams *et al.* reported no significant difference of hippocampus volume between glaucoma and controls, but an increase in hippocampus volume with disease severity in patients with glaucoma[22].

Such differences between study results may be explained by differences in study methodology, in particular regarding the selection of subjects and severity of the disease, MRI sequences used or definition of regions of interest. For instance, in a recent study by Frezzotti et al, only severe cases of glaucoma (but not early) showed grey matter atrophy of the visual cortex and hippocampus[47]. The evolution of brain volume in the course of glaucoma and its association with other neurodegenerative diseases would need further investigation and prospective follow-up of subjects. Finally, functional MRI may offer new insights into the brain modifications associated

with glaucoma, as suggested by two recent studies, showing functional modifications of the visual cortex at the earliest stages of the disease[47,48].

In conclusion, we confirmed microstructural changes of optic radiations in glaucoma and its association with glaucoma severity. In accordance with several other studies, DTI appears as an objective measurement for evaluating alterations of the visual pathways in glaucoma and provides new insight in the pathophysiological process of glaucoma. A prospective evaluation of our cohort of patients would be of interest to observe the evolution of these microstructural modifications of optic radiations and to analyze the evolution of brain volume in association with the evolution of glaucoma disease. DTI could represent a future way to explore central nervous system of glaucomatous subjects, leading to a better understanding of the pathophysiology and, potentially, to help clinical trials evaluate new therapeutic strategies based on neuroprotection or brain repair.

REFERENCES

1. Resnikoff S, Pascolini D, Etya'ale D, et al. Global data on visual impairment in the year 2002. *Bull World Health Organ*. 2004;82(11):844-851. doi:/S0042-96862004001100009.
2. Tham Y-C, Li X, Wong TY, Quigley HA, Aung T, Cheng C-Y. Global prevalence of glaucoma and projections of glaucoma burden through 2040: a systematic review and meta-analysis. *Ophthalmology*. 2014;121(11):2081-2090. doi:10.1016/j.ophtha.2014.05.013.
3. Weinreb RN, Khaw PT. Primary open-angle glaucoma. *Lancet*. 2004;363(9422):1711-1720. doi:10.1016/S0140-6736(04)16257-0.
4. O'Hare F, Rance G, McKendrick AM, Crowston JG. Is primary open-angle glaucoma part of a generalized sensory neurodegeneration? A review of the evidence. *Clin Experiment Ophthalmol*. 2012;40(9):895-905. doi:10.1111/j.1442-

9071.2012.02812.x.
5. Gupta N, Yücel YH. Glaucoma as a neurodegenerative disease. *Curr Opin Ophthalmol*. 2007;18(2):110-114. doi:10.1097/ICU.0b013e3280895aea.
6. Yucel YH, Gupta N. A framework to explore the visual brain in glaucoma with lessons from models and man. *Exp Eye Res*. 2015;141:171-178. doi:10.1016/j.exer.2015.07.004.
7. Yücel Y. Central nervous system changes in glaucoma. *J Glaucoma*. 2013;22 Suppl 5:S24-25. doi:10.1097/IJG.0b013e3182934a55.
8. Zhang S, Wang H, Lu Q, et al. Detection of early neuron degeneration and accompanying glial responses in the visual pathway in a rat model of acute intraocular hypertension. *Brain Res*. 2009;1303:131-143. doi:10.1016/j.brainres.2009.09.029.
9. Boucard CC, Hernowo AT, Maguire RP, et al. Changes in cortical grey matter density associated with long-standing retinal visual field defects. *Brain J Neurol*. 2009;132(Pt 7):1898-1906. doi:10.1093/brain/awp119.
10. Gupta N, Ang L-C, Noël de Tilly L, Bidaisee L, Yücel YH. Human glaucoma and neural degeneration in intracranial optic nerve, lateral geniculate nucleus, and visual cortex. *Br J Ophthalmol*. 2006;90(6):674-678. doi:10.1136/bjo.2005.086769.
11. Gupta N, Greenberg G, de Tilly LN, Gray B, Polemidiotis M, Yücel YH. Atrophy of the lateral geniculate nucleus in human glaucoma detected by magnetic resonance imaging. *Br J Ophthalmol*. 2009;93(1):56-60. doi:10.1136/bjo.2008.138172.
12. Zhang YQ, Li J, Xu L, et al. Anterior visual pathway assessment by magnetic resonance imaging in normal-pressure glaucoma. *Acta Ophthalmol (Copenh)*. 2012;90(4):e295-302. doi:10.1111/j.1755-3768.2011.02346.x.
13. Zikou AK, Kitsos G, Tzarouchi LC, Astrakas L, Alexiou GA, Argyropoulou MI. Voxel-based morphometry and diffusion tensor imaging of the optic pathway in primary open-angle glaucoma: a preliminary study. *AJNR Am J Neuroradiol*. 2012;33(1):128-134. doi:10.3174/ajnr.A2714.
14. Chen WW, Wang N, Cai S, et al. Structural Brain Abnormalities in Patients with Primary Open-Angle Glaucoma: A Study with 3T MR Imaging. *Investig Opthalmology Vis Sci*. 2013;54(1):545. doi:10.1167/iovs.12-9893.
15. Dai H, Mu KT, Qi JP, et al. Assessment of lateral geniculate nucleus atrophy with 3T MR imaging and correlation with clinical stage of glaucoma. *AJNR Am J Neuroradiol*. 2011;32(7):1347-1353. doi:10.3174/ajnr.A2486.
16. Chan KC, Fu Q, Hui ES, So K, Wu EX. Evaluation of the retina and optic nerve in a rat model of chronic glaucoma using in vivo manganese-enhanced magnetic resonance imaging. *NeuroImage*. 2008;40(3):1166-1174. doi:10.1016/j.neuroimage.2008.01.002.
17. Chan KC, So K, Wu EX. Proton magnetic resonance spectroscopy revealed choline reduction in the visual cortex in an experimental model of chronic glaucoma. *Exp Eye Res*. 2009;88(1):65-70. doi:10.1016/j.exer.2008.10.002.
18. Ho LC, Wang B, Conner IP, et al. In Vivo Evaluation of White Matter Integrity and Anterograde Transport in Visual System After Excitotoxic Retinal Injury With Multimodal MRI and OCT. *Invest Ophthalmol Vis Sci*. 2015;56(6):3788-3800. doi:10.1167/iovs.14-15552.
19. Helmer C, Malet F, Rougier M-B, et al. Is there a link between open-angle glaucoma and dementia?: The Three-City-Alienor Cohort. *Ann Neurol*. May 2013. doi:10.1002/ana.23926.
20. Lin I-C, Wang Y-H, Wang T-J, et al. Glaucoma, Alzheimer's disease, and

Parkinson's disease: an 8-year population-based follow-up study. *PloS One*. 2014;9(9):e108938. doi:10.1371/journal.pone.0108938.
21. Frezzotti P, Giorgio A, Motolese I, et al. Structural and functional brain changes beyond visual system in patients with advanced glaucoma. *PloS One*. 2014;9(8):e105931. doi:10.1371/journal.pone.0105931.
22. Williams AL, Lackey J, Wizov SS, et al. Evidence for widespread structural brain changes in glaucoma: a preliminary voxel-based MRI study. *Invest Ophthalmol Vis Sci*. 2013;54(8):5880-5887. doi:10.1167/iovs.13-11776.
23. Le Bihan D, Iima M. Diffusion Magnetic Resonance Imaging: What Water Tells Us about Biological Tissues. *PLoS Biol*. 2015;13(7):e1002203. doi:10.1371/journal.pbio.1002203.
24. El-Rafei A, Engelhorn T, Wärntges S, Dörfler A, Hornegger J, Michelson G. A framework for voxel-based morphometric analysis of the optic radiation using diffusion tensor imaging in glaucoma. *Magn Reson Imaging*. 2011;29(8):1076-1087. doi:10.1016/j.mri.2011.02.034.
25. Garaci FG, Bolacchi F, Cerulli A, et al. Optic nerve and optic radiation neurodegeneration in patients with glaucoma: in vivo analysis with 3-T diffusion-tensor MR imaging. *Radiology*. 2009;252(2):496-501. doi:10.1148/radiol.2522081240.
26. Chen Z, Lin F, Wang J, et al. Diffusion tensor magnetic resonance imaging reveals visual pathway damage that correlates with clinical severity in glaucoma. *Clin Experiment Ophthalmol*. 2013;41(1):43-49. doi:10.1111/j.1442-9071.2012.02832.x.
27. Folstein MF, Folstein SE, McHugh PR. "Mini-mental state". A practical method for grading the cognitive state of patients for the clinician. *J Psychiatr Res*. 1975;12(3):189-198.
28. Maeda N, Klyce SD, Smolek MK, Thompson HW. Automated keratoconus screening with corneal topography analysis. *Invest Ophthalmol Vis Sci*. 1994;35(6):2749-2757.
29. Reich DS, Smith SA, Gordon-Lipkin EM, et al. Damage to the optic radiation in multiple sclerosis is associated with retinal injury and visual disability. *Arch Neurol*. 2009;66(8):998-1006. doi:10.1001/archneurol.2009.107.
30. Wakana S, Jiang H, Nagae-Poetscher LM, van Zijl PCM, Mori S. Fiber tract-based atlas of human white matter anatomy. *Radiology*. 2004;230(1):77-87. doi:10.1148/radiol.2301021640.
31. Wheeler-Kingshott C a. M, Trip SA, Symms MR, Parker GJM, Barker GJ, Miller DH. In vivo diffusion tensor imaging of the human optic nerve: pilot study in normal controls. *Magn Reson Med*. 2006;56(2):446-451. doi:10.1002/mrm.20964.
32. Manjón JV, Coupé P, Martí-Bonmatí L, Collins DL, Robles M. Adaptive non-local means denoising of MR images with spatially varying noise levels. *J Magn Reson Imaging JMRI*. 2010;31(1):192-203. doi:10.1002/jmri.22003.
33. Avants BB, Tustison NJ, Song G, Cook PA, Klein A, Gee JC. A reproducible evaluation of ANTs similarity metric performance in brain image registration. *NeuroImage*. 2011;54(3):2033-2044. doi:10.1016/j.neuroimage.2010.09.025.
34. Manjón JV, Eskildsen SF, Coupé P, Romero JE, Collins DL, Robles M. Nonlocal intracranial cavity extraction. *Int J Biomed Imaging*. 2014;2014:820205. doi:10.1155/2014/820205.
35. Coupé P, Manjón JV, Fonov V, Pruessner J, Robles M, Collins DL. Patch-based segmentation using expert priors: application to hippocampus and ventricle segmentation. *NeuroImage*. 2011;54(2):940-954. doi:10.1016/j.neuroimage.2010.09.018.

36. Frisoni GB, Jack CR, Bocchetta M, et al. The EADC-ADNI Harmonized Protocol for manual hippocampal segmentation on magnetic resonance: evidence of validity. *Alzheimers Dement J Alzheimers Assoc*. 2015;11(2):111-125. doi:10.1016/j.jalz.2014.05.1756.
37. Sowmya V, Venkataramanan VR, Prasad V. Effect of Refractive Status and Axial Length on Peripapillary Retinal Nerve Fibre Layer Thickness: An Analysis Using 3D OCT. *J Clin Diagn Res JCDR*. 2015;9(9):NC01-04. doi:10.7860/JCDR/2015/14112.6480.
38. Murai H, Suzuki Y, Kiyosawa M, Tokumaru AM, Ishii K, Mochizuki M. Positive correlation between the degree of visual field defect and optic radiation damage in glaucoma patients. *Jpn J Ophthalmol*. February 2013. doi:10.1007/s10384-013-0233-0.
39. Engelhorn T, Michelson G, Waerntges S, et al. A new approach to assess intracranial white matter abnormalities in glaucoma patients: changes of fractional anisotropy detected by 3T diffusion tensor imaging. *Acad Radiol*. 2012;19(4):485-488. doi:10.1016/j.acra.2011.12.005.
40. Michelson G, Engelhorn T, Wärntges S, El Rafei A, Hornegger J, Doerfler A. DTI parameters of axonal integrity and demyelination of the optic radiation correlate with glaucoma indices. *Graefes Arch Clin Exp Ophthalmol Albrecht Von Graefes Arch Für Klin Exp Ophthalmol*. 2013;251(1):243-253. doi:10.1007/s00417-011-1887-2.
41. Pietrasanta M, Restani L, Caleo M. The Corpus Callosum and the Visual Cortex: Plasticity Is a Game for Two. *Neural Plast*. 2012;2012:1-10. doi:10.1155/2012/838672.
42. Strouthidis NG, Fortune B, Yang H, Sigal IA, Burgoyne CF. Longitudinal change detected by spectral domain optical coherence tomography in the optic nerve head and peripapillary retina in experimental glaucoma. *Invest Ophthalmol Vis Sci*. 2011;52(3):1206-1219. doi:10.1167/iovs.10-5599.
43. Tan O, Chopra V, Lu AT-H, et al. Detection of macular ganglion cell loss in glaucoma by Fourier-domain optical coherence tomography. *Ophthalmology*. 2009;116(12):2305-2314.e1-2. doi:10.1016/j.ophtha.2009.05.025.
44. Yang Y, Zhang H, Yan Y, Gui Y, Zhu T. Comparison of optic nerve morphology in eyes with glaucoma and eyes with non-arteritic anterior ischemic optic neuropathy by Fourier domain optical coherence tomography. *Exp Ther Med*. 2013;6(1):268-274. doi:10.3892/etm.2013.1115.
45. Jonas RA, Wang YX, Yang H, et al. Optic Disc - Fovea Angle: The Beijing Eye Study 2011. *PloS One*. 2015;10(11):e0141771. doi:10.1371/journal.pone.0141771.
46. Chang EE, Goldberg JL. Glaucoma 2.0: Neuroprotection, Neuroregeneration, Neuroenhancement. *Ophthalmology*. 2012;119(5):979-986. doi:10.1016/j.ophtha.2011.11.003.
47. Murphy MC, Conner IP, Teng CY, et al. Retinal Structures and Visual Cortex Activity are Impaired Prior to Clinical Vision Loss in Glaucoma. *Sci Rep*. 2016;6:31464. doi:10.1038/srep31464.
48. Frezzotti P, Giorgio A, Toto F, De Leucio A, De Stefano N. Early changes of brain connectivity in primary open angle glaucoma. *Hum Brain Mapp*. August 2016. doi:10.1002/hbm.23330.

Figure 1. Building of optic radiations and measurement of fractional anisotropy, using the Olea Medical ® software (image: CHU de Bordeaux, department of neuroimaging).

Green boxes are the markers placed manually on anterior and posterior parts of the optic radiations. Green lines are optic radiations automatically reconstructed by the Olea Medical® software. Red boxes are markers manually placed to manually deleted fibers outside the expected area.

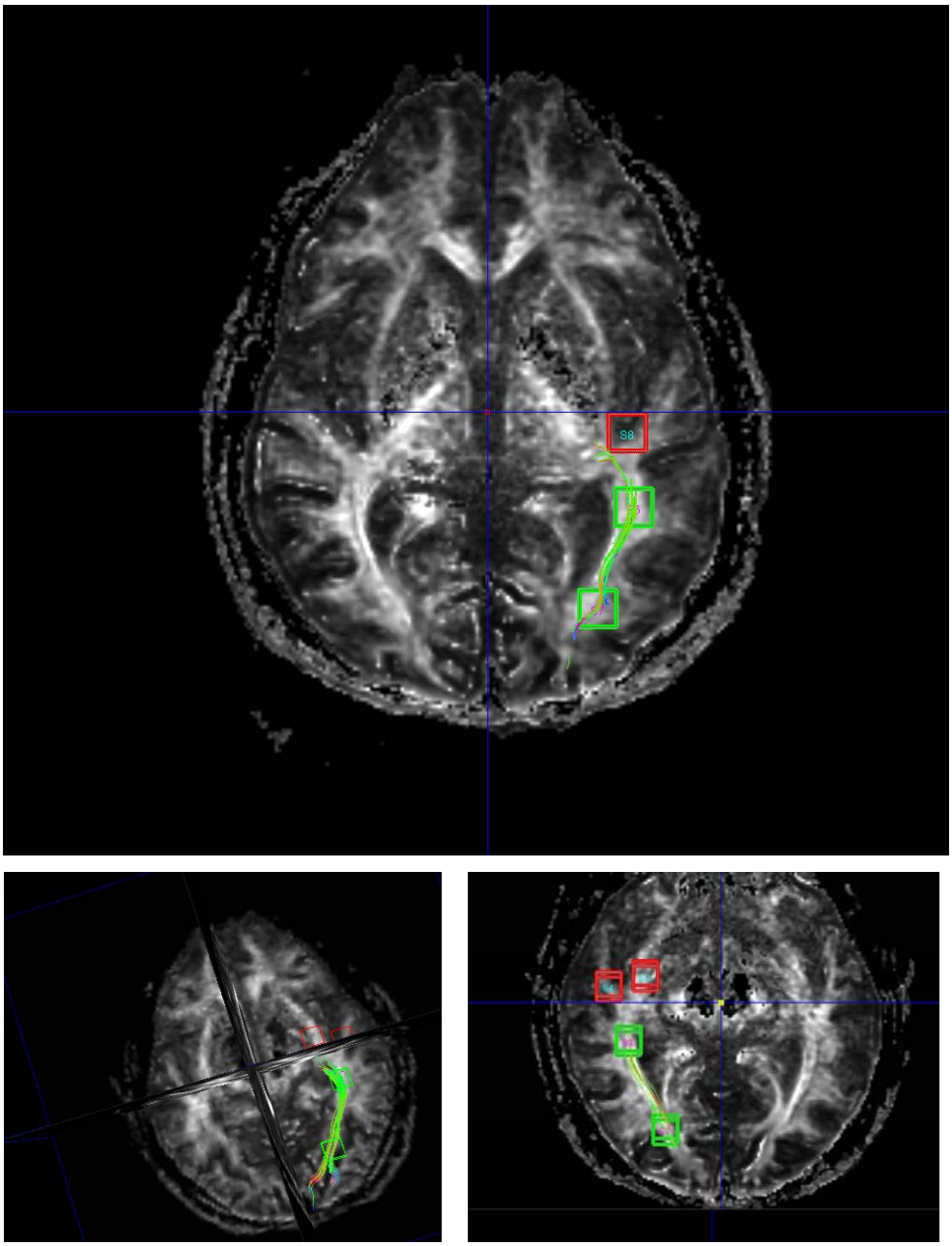

Table 1: General characteristics

Characteristics	Glaucoma (n=50)	Control (n=50)	p-value*
Age (years, mean(SD))	61.9 (6.9)	61.9 (7.0)	0.98
Sex (n, %)			1
Male	20 (40)	20 (40)	
Female	30 (60)	30 (60)	
MMSE (mean(SD))	29.3 (0.8)	29.4 (0.8)	0.7
Family history of glaucoma (n (%))			<0.0001
Yes	29 (58)	0 (0)	
No	16 (32)	50 (100)	
Unknown	5 (10)	0 (0)	
Self-reported medical history			
Hypertension (n (%))	11 (22)	12 (24)	0.81
Hypercholesterolemia (n (%))	14 (28)	12 (24)	0.65
Hypertriglyceridemia (n (%))	2 (4)	3 (6)	0.65
Myocardial infarction (n (%))	2 (4)	1 (2)	0.56
Smoking (n (%))			0.67
Never	29 (58)	25 (50)	
Former	17 (34)	19 (38)	
Current	4 (8)	6 (12)	

MMSE: Mini Mental State Examination
* Chi-square for categorical variables and Student t-test for continuous variables

Table 2: Ophthalmological characteristics; right eye (mean (standard deviation))

Characteristics	Glaucoma (n=50)	Control (n=50)	p-value*
Best-Corrected Visual Acuity (logMAR)			
Distance	0.03 (0.09)	0.006 (0.02)	0.09
Near	0.19 (0.07)	0.18 (0.00)	0.2
Central corneal thickness (µm)	525.9 (30.9)	544.0[1] (31.9)	0.005
Axial Length (mm)	24.1 (1.1)	23.7 (1.2)	0.15
IOP (mmHg)	14.6 (3.7)	14.7 (2.5)	0.82
Vertical Cup : Disc Ratio	0.8 (0.2)[1]	0.3 (0.2)[1]	<0.0001
RNFL Thickness (µm)	76.9 (17.7)	93.2 (9.9)	<0.0001
Visual field (dB)			
Mean Sensitivity	21.9 (6.1)	26.6 (1.1)	<0.0001
Mean Deviation	5.0 (6.0)	0.3 (1.0)	<0.0001
Loss Variance	22.6 (26.3)	5.0 (1.8)	<0.0001

RNFL: Retinal Nerve Fiber Layer

IOP: Intraocular Pressure

* Chi-square for categorical variables and Student t-test for continuous variables

[1] One missing data

Table 3: Ophthalmological characteristics; left eye (mean (standard deviation))

Characteristics	Glaucoma (n=50)	Control (n=50)	p-value*
Best-Corrected Visual Acuity (logMAR)			
Far	0.03 (0.08)	0.006 (0.02)	0.08
Near	0.2 (0.1)	0.2 (0)	0.1
Central corneal thickness (µm)	524.6 (30.0)[1]	542.9 (28.4)[2]	0.003
Axial Length (mm)	24.0 (1.0)	23.5 (0.8)	0.003
IOP (mmHg)	14.2 (3.2)	15.2 (2.4)	0.09
Vertical Cup : Disc Ratio			
Funduscopy	0.8 (0.2)	0.3 (0.2)	<0.0001
RNFL Thickness (µm)	70.1 (18.7)	93.1 (9.7)	<0.0001
Visual field (dB)			
Mean Sensitivity: MS	21.8 (4.6)	26.6 (1.2)	<0.0001
Mean Deviation: MD	5.1 (4.5)	0.3 (1.1)	<0.0001
Loss Variance: LV	28.1 (28.0)	4.7 (2.2)	<0.0001

RNFL: Retinal Nerve Fiber Layer
IOP: Intraocular Pressure
* Chi-square for categorical variables and Student t-test for continuous variables
[1] One missing data[2] Two missing data

Table 4: Comparison of MRI parameters along optic radiations between glaucoma and control subjects (mean (standard deviation))

	Glaucoma (n=49)	**Control** (n=47)	**P-value***
Fractional anisotropy	0.57 (0.04)	0.59 (0.03)	0.02
Mean diffusivity (10^{-5} mm^2/s)	82.38 (6.43)	80.62 (4.87)	0.10
Axial diffusivity (10^{-5} mm^2/s)	141.59 (7.14)	142.37 (6.74)	0.53
Radial diffusivity (10^{-5} mm^2/s)	52.78 (6.74)	49.74 (5.04)	0.03
Length (mm)	63.91 (6.80)	63.72 (7.15)	0.74
Volume (cm^3)	20.79 (9.13)	24.96 (12.33)	0.11

*P-value: logistic conditional analyses

Table 5: Associations of homo- and contra-lateral optic radiation parameters with the severity of the disease in glaucoma patients

	Visual field Mean Deviation		Funduscopy Vertical Cup/Disc Ratio		SD-OCT examination RNFL thickness	
	β[95%CI]	**P**	**β [95%CI]**	**P**	**β [95%CI]**	**P**
Homolateral						
Fractional anisotropy	-0.22 [-0.41;-0.02]	**0.03**	-0.42 [-0.64;-0.21]	**0.0003**	0.22 [0.03;0.41]	**0.03**
Mean diffusivity	0.02 [-0.17;0.21]	0.80	0.29 [0.08;0.50]	**0.008**	-0.15 [-0.34;0.04]	0.12
Axial diffusivity	-0.11 [-0.31;0.08]	0.26	0.09 [-0.14;0.31]	0.45	-0.06 [-0.26;0.14]	0.56
Radial diffusivity	0.09 [-0.10;0.28]	0.33	0.38 [0.17;0.59]	**0.0006**	-0.18 [-0.37;-0.007]	0.06
Controlateral						
Fractional anisotropy	-0.17 [-0.37;0.02]	0.09	-0.28 [-0.55;-0.06]	**0.01**	0.10 [-0.09;0.30]	0.30
Mean diffusivity	0.13 [-0.06;0.31]	0.19	0.20 [-0.02;0.41]	0.07	0.01 [-0.18;0.21]	0.91
Axial diffusivity	0.04 [-0.15;0.24]	0.67	0.07 [-0.16;0.30]	0.55	0.09 [-0.11;0.30]	0.34
Radial diffusivity	0.15 [-0.04;0.34]	0.11	0.25 [0.04;0.46]	**0.02**	-0.03 [-0.23;0.16]	0.72

CI: Confidence Interval; RNFL: Retinal Nerve Fiber Layer
P-value adjusted for age and gender, with additional adjustment for axial length for RNFL

Table 6: Comparison of DTI parameters and MRI-based volume between glaucoma and control subjects (mean (standard deviation))

	Cerebrum white matter			Cerebrum grey matter			Hippocampus			Amygdala		
	Glaucoma	Control	P-value*	Glaucoma	Control	P-value	Glaucoma	Control	P-value	Glaucoma	Control	P-value
	(n=48)	(n=48)		(n=48)	(n=48)		(n=48)	(n=48)		(n=48)	(n=48)	
Volume (cm^3)	275.28 (115.61)	238.25 (59.03)	0.06	270.19 (59.03)	283.09 (38.17)	0.18	3.95 (0.53)	3.84 (0.46)	0.16	0.60 (0.23)	0.55 (0.18)	0.22
DTI parameters	(n=41)	(n=41)		(n=41)	(n=41)		(n=41)	(n=41)		(n=41)	(n=41)	
FA	0.38 (0.02)	0.37 (0.02)	0.39	0.17 (0.01)	0.17 (0.01)	0.45	0.19 (0.01)	0.19 (0.02)	0.44	0.15 (0.02)	0.15 (0.01)	0.09
MD (10^{-5} mm^2/s)	78.34 (3.58)	78.19 (3.21)	0.79	121.70 (9.63)	120.01 (8.81)	0.25	98.83 (8.82)	97.72 (5.79)	0.42	80.45 (4.03)	80.56 (3.40)	0.87
AD (10^{-5} mm^2/s)	110.91 (2.80)	110.35 (2.53)	0.26	138.84 (10.50)	136.96 (9.67)	0.24	116.86 (9.78)	115.46 (6.17)	0.39	92.64 (4.43)	92.21 (3.31)	0.57
RD (10^{-5} mm^2/s)	62.24 (4.17)	62.27 (3.78)	0.96	113.20 (9.23)	111.60 (8.44)	0.26	90.02 (8.40)	88.90 (5.74)	0.44	74.35 (3.99)	74.73 (3.53)	0.57

Abreviations: AD: Axial diffusivity; FA: Fractional anisotropy; MD: Mean diffusivity; RD: Radial diffusivity

*P-value : logistic conditional analyses